# The combined effects of ENSO and the 11 year solar cycle on the Northern Hemisphere polar stratosphere

Natalia Calvo[1,2] and Daniel R. Marsh[1]

Received 20 October 2010; revised 13 October 2011; accepted 14 October 2011; published 13 December 2011.

[1] The combined effects of El Niño–Southern Oscillation (ENSO) and the 11 year solar cycle on the Northern Hemisphere polar stratosphere have been analyzed in the Whole Atmosphere Community Climate Model version 3 in the absence of the quasi-biennial oscillation. The polar response to ENSO agrees with previous studies during solar minimum; composites of warm minus cold ENSO events show a warmer polar stratosphere and a weaker polar vortex, propagating downward as the winter evolves. During solar maximum conditions, little downward propagation of the ENSO signal is simulated, leading to colder temperatures and stronger winds in the polar lower stratosphere. The analysis of the Eliassen-Palm flux and wave index of refraction shows that this is mainly due to a reduction of upward propagating extratropical planetary wave number 1 component caused by changes in the background winds in the subtropics related to a warmer tropical upper stratosphere during solar maximum. The effect of the 11 year solar cycle variability on the polar stratosphere is not significant during cold ENSO events until February. During warm ENSO events, a statistically significant colder polar lower stratosphere and stronger polar vortex are simulated throughout the winter, and no downward propagation of this signal occurs. This is mainly due to the combined effects of solar maximum and warm ENSO conditions on the wave mean flow interaction. These results show a nonlinear behavior of the extratropical stratosphere response to the combination of the two forcings and highlight the need to stratify with respect to ENSO and solar conditions and analyze the seasonal march throughout the winter.

**Citation:** Calvo, N., and D. R. Marsh (2011), The combined effects of ENSO and the 11 year solar cycle on the Northern Hemisphere polar stratosphere, *J. Geophys. Res.*, *116*, D23112, doi:10.1029/2010JD015226.

## 1. Introduction

[2] El Nino–Southern Oscillation (ENSO) originates in the tropical troposphere as a coupled ocean-atmosphere phenomenon. Its signal propagates upward into the stratosphere where different observational data sets have shown its effect on the Northern Hemisphere (NH) polar region [*van Loon and Labitzke*, 1987; *Hamilton*, 1993; *Camp and Tung*, 2007; *Free and Seidel*, 2009]. In the last decade, several works have used general circulation models to isolate the ENSO signal from other sources of variability, which are important in the stratosphere and thus, increase our understanding of how ENSO affected the polar stratosphere [*Sassi et al.*, 2004; *Manzini et al.*, 2006; *García-Herrera et al.*, 2006; *Calvo et al.*, 2008; *Cagnazzo et al.*, 2009]. They showed that warm ENSO events cause anomalous propagation and dissipation of planetary Rossby waves at middle latitudes. These anomalies weaken the westerly background flow and strengthen the stratospheric branch of the Brewer-Dobson circulation toward the North Pole, which in turn generates anomalous warming in the polar vortex. The effect of cold ENSO events on the Northern Hemisphere polar region is however ambiguous. For instance, *García-Herrera et al.* [2006] obtained an opposite but much weaker effect (i.e., a stronger polar vortex accompanied by a colder polar stratosphere, not shown) while *Manzini et al.* [2006] did not find a significant polar response to a cold event.

[3] The quasi-biennial oscillation (QBO) also contributes to the variability of the NH polar vortex. The alternation of westerly and easterly winds in the tropics and the associated secondary meridional circulation modify the regions where the planetary waves can propagate and dissipate at mid-latitudes. As a consequence, anomalies in the stratospheric branch of the Brewer-Dobson circulation in the NH polar region are produced and polar zonal mean temperature and wind patterns are modified. A colder and stronger polar vortex is observed during the westerly QBO phase while the opposite occurs during the easterly phase. This is known as the Holton and Tan relationship and has been found in both models and observations [*Holton and Tan*, 1980, 1982; *Baldwin et al.*, 2001; *Calvo et al.*, 2007].

[1]Atmospheric Chemistry Division, National Center for Atmospheric Research, Boulder, Colorado, USA.
[2]Departamento de Física de la Tierra II, Universidad Complutense de Madrid, Madrid, Spain.


0148-0227/11/2010JD015226

**Table 1.** Winters Considered During the 1950–2004 Period in the Four Composites Computed in This Study[a]

| | Cold ENSO Events | Warm ENSO Events |
|---|---|---|
| Solar minimum conditions | 1973–1974 | 1965–1966 |
| | 1975–1976 | 1972–1973 |
| | 1984–1985 | 1986–1987 |
| | | 1997–1998 |
| Solar maximum conditions | 1970–1971 | 1957–1958 |
| | 1988–1989 | 1968–1969 |
| | 1999–2000 | 1982–1983 |
| | | 1991–1992 |

[a]Note that each composite had three 55 year simulations; therefore, each composite has three times the winters shown.

[4] Changes in solar irradiance over the 11 year solar cycle are known to cause temperature anomalies in the upper tropical stratosphere [*Hood*, 2004; *Marsh et al.*, 2007]. This pattern modifies the meridional gradient of temperature and thus the mean wind, which could eventually affect the wave mean flow interaction and the stratospheric NH polar region. However, several studies have shown that the solar signal in the polar stratosphere is only noticeable when it is combined with either strong westerly or easterly QBO phases [*Labitzke and van Loon*, 1988; *Gray et al.*, 2001].

[5] In fact, the response of the polar stratosphere to a combination of two different external forcings has been the focus of several recent studies. In addition to the aforementioned influence of the QBO on the intensification of the solar response in the extratropics, the QBO also interacts with the extratropical signal of ENSO [*Garfinkel and Hartmann*, 2007; *Calvo et al.*, 2009], modifying its temporal evolution and amplitude in the NH polar region. For instance, *Calvo et al.* [2009] showed that the effects of ENSO on the polar vortex are intensified during both QBO phases at the end of the boreal winter while their onset does depend on the phase of the QBO. In turn, ENSO also has an impact on the extratropical signal of the QBO. *Wei et al.* [2007] found a much weaker QBO response in the polar stratosphere during warm ENSO events compared to cold ENSO events while *Calvo et al.* [2009] showed that warm ENSO events accelerate the downward propagation of the extratropical QBO signal in late winter leading to a weaker signal in the polar region. These signals are the result of changes in the interaction between the upward propagating waves and the background flow. It is interesting to note that the response of the polar stratosphere to the combined effect of both a warm ENSO event and the easterly phase of the QBO (both of which act to perturb the polar vortex when they operate independently) is nonadditive, and the resulting perturbation of the polar vortex is smaller than the addition of the two independent responses.

[6] Recent results have shown that the extratropical signal of ENSO also depends on the phase of the 11 year solar cycle. *Kryjov and Park* [2007] analyzed the ENSO signal in the polar stratosphere during boreal winter in NCEP/NCAR reanalysis data and showed that the ENSO signal is only observed during solar minimum conditions. However, no dynamical mechanism was given to explain this behavior. *Kuroda* [2007] studied the relationship between stratospheric winds and the North Atlantic Oscillation (NAO), and its dependence on solar, QBO and ENSO forcing using ERA-40 data. They found that the modulation of the NAO by the solar signal is amplified during cold ENSO events and west QBO phases. Nevertheless, some uncertainties remain in their studies. They both used observational reanalysis data sets, which include other sources of variability (e.g., QBO) that can complicate the analysis of the response in the stratosphere, as the authors themselves pointed out.

[7] Our study makes use of version 3 of the Whole Atmosphere Community Climate Model (WACCM3) [*Garcia et al.*, 2007] to analyze both the solar cycle modulation of the ENSO signal (as observed in reanalysis by *Kryjov and Park* [2007]) and the ENSO effect on the solar cycle response in the NH stratospheric polar region. Because WACCM3 does not spontaneously generate a QBO, and one was not prescribed in the experiments used here, it is possible to calculate the net effect of one phenomenon on the other without the presence of QBO variability. As mentioned above, the QBO is known to interact nonlinearly with both ENSO and the 11 year solar cycle signal and so would complicate the analysis of model simulations. In this sense, this is a "cleaner" experiment, in which to investigate interactions between ENSO and solar cycle.

## 2. Model Simulations and Method

[8] WACCM3 is a coupled chemistry climate model developed at the National Center for Atmospheric Research (NCAR) based on the Community Atmospheric Model (CAM3) [*Collins et al.*, 2004]. The processes and parameterizations that are unique to WACCM3 are described by *Garcia et al.* [2007] and *Marsh et al.* [2007]. The model spans from the surface up to the thermosphere ($\sim$140 km) with horizontal resolution of 1.9° latitude versus 2.5° longitude. Sea surface temperatures, surface concentrations of greenhouse gases and halogen species were specified from observations. The 11 year solar cycle spectral irradiance variability was parameterized in terms of the observed 10.7 cm radio flux (f10.7). Our version of the model used here differs from the one used in CCMVal1 in its horizontal spatial resolution (4° latitude versus longitude was used for CCMVal1).

[9] This study analyzes a 3 member ensemble of WACCM3 simulation from 1950 to 2004. For each ensemble member the monthly mean temperature and zonal mean zonal wind time series were detrended and the ensemble mean for each month removed. Monthly composites for warm and cold ENSO (wEN and cEN) and solar maximum (Smax) and minimum (Smin) conditions were then computed for boreal winter months. The Niño 3.4 index (N3.4, from the Climate Prediction Center; http://www.cpc.noaa.gov/data/indices) has been used to stratify with respect to ENSO: warm and cold events were defined when the winter average (December-January-February, DJF) of the normalized N3.4 exceeds 1 or $-1$ standard deviation. The 11 year solar cycle has been characterized using the f10.7 index: boreal winters were classified as Smax when the DJF average of the f10.7 index exceeds 145 solar flux units and Smin when the index is lower than 100. Thus, four different composites have been obtained: wENSmax, cENSmax, wENSmin and cENSmin. Table 1 shows the winters chosen for each category.

[10] The significance of the composited anomalies with respect to internal natural variability was assessed through a Monte Carlo test following the methodology of *García-*

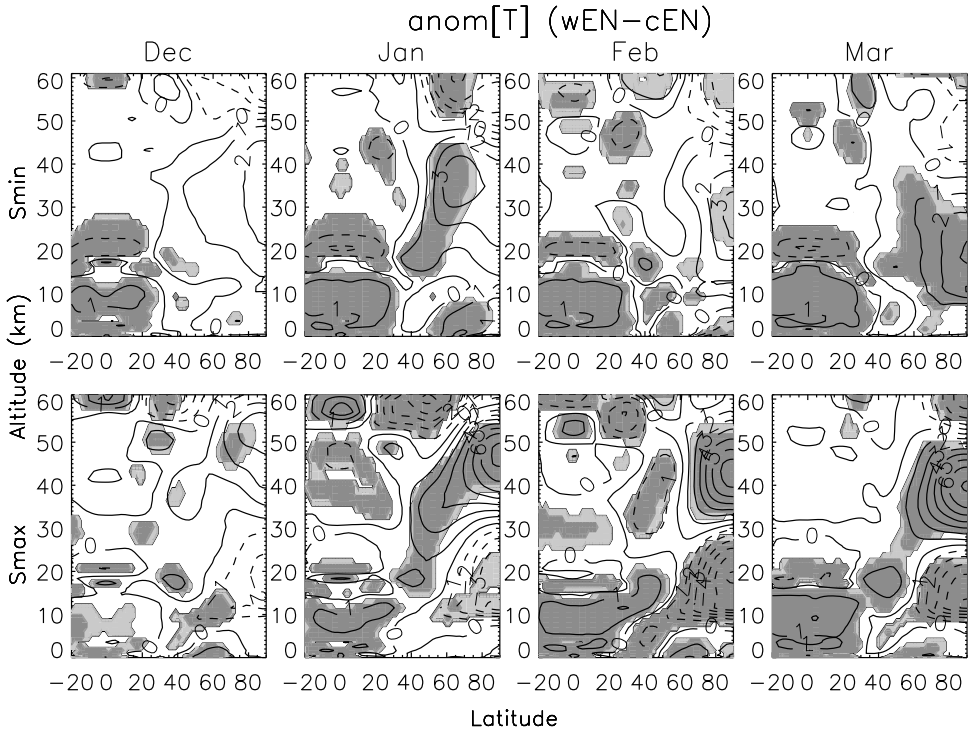


**Figure 1.** Detrended zonal mean temperature anomalies composited for (top) the warm minus cold ENSO events difference during Smin conditions (wEN − cEN Smin) and (bottom) wEN − cEN during Smax conditions from December (first column) to March (fourth column). Contours are drawn every 1 K. Dashed contours denote negative values. Significant anomalies computed through a Monte Carlo test (see text for more details) are shadowed in light (dark) gray for 90% (95%) significance levels. Vertical coordinate is log-pressure altitude.

*Herrera et al.* [2006]. Random groups of the same number of months considered in the composites were used to compute random composites. These random composites consider the fact that we use three 55 year simulations instead of a single 165 year simulation. Random composites were computed 1000 times to obtain a stable Gaussian probability distribution. This distribution has the 5% (10%) tails (2.5% or 5% each tail at each side) approximately at $\pm 1.96$ ($\pm 1.64$) standard deviations from the mean. Composite anomalies that exceed these thresholds are considered significant.

## 3. Results

### 3.1. Impact of the 11 Year Solar Cycle on the ENSO Signal

[11] Figure 1 shows the warm minus cold ENSO events (wEN − cEN) composite differences for each month of the zonal mean temperature field. From left to right, Figure 1 shows the temporal evolution from December to March during Smin (Figure 1, top) conditions and Smax (Figure 1, bottom) conditions, respectively. In the tropics, anomalous zonal mean warming and cooling is simulated in the troposphere and lower stratosphere during Smin conditions, in agreement with previous studies that analyzed the ENSO signal in this area in both observations and models [e.g., *Randel et al.*, 2009; *Calvo et al.*, 2010]. During Smax (Figure 1, bottom), the tropical ENSO signal is very similar to the one observed during Smin conditions although the anomalous cooling in the lower stratosphere seems more confined to its lowermost part and the anomalous tropospheric warming is weaker in early winter (December and January).

[12] In the Northern Hemisphere high latitudes, during solar minimum conditions, (wEN − cEN) Smin, significant warm anomalies are observed in the polar stratosphere, from January to March, with cold anomalies above them in the upper stratosphere and lower mesosphere region. The dipole structure is in good agreement with previous observational studies that dealt with the ENSO response in the NH polar region without discriminating with respect to the phase of the solar cycle [e.g., *van Loon and Labitzke*, 1987], and also with model studies where the solar cycle variability was not included [*Sassi et al.*, 2004; *García-Herrera et al.*, 2006]. Anomalous values reach up to 3 K throughout the winter. The downward propagation of the ENSO signal as the winter evolves, which was first described by *Manzini et al.* [2006], is well reproduced in WACCM.

[13] During Smax, the ENSO composites show an anomalously cold polar vortex below 30 km, which is significant from January to March. A significant warming also appears in the upper stratosphere. This dipole pattern resembles the one observed during Smin but of opposite sign. However, it is clear from the seasonal march of the differences that during Smax conditions, warm anomalies in the polar region are located in the middle and upper stratosphere (reaching up to 6–7 K from January to March, much stronger than during Smin conditions). Unlike during Smin conditions, the anomalous warming never descends into the lower stratosphere. The anomalies in temperature are accompanied by

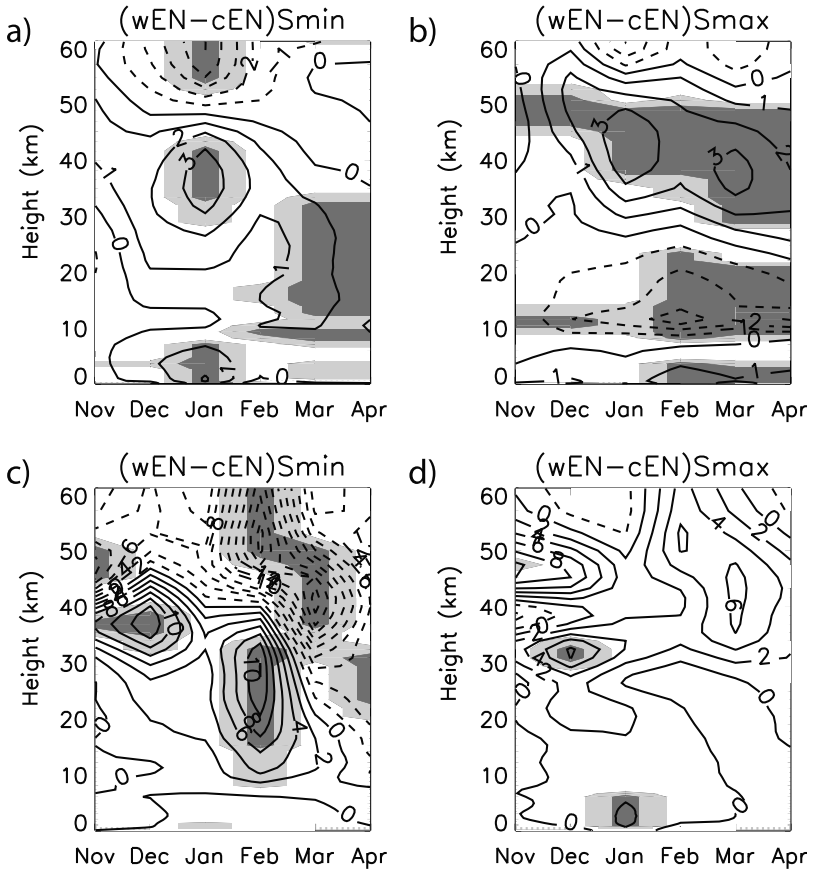


**Figure 2.** Time-log P altitude cross section of zonal mean temperature anomalies at 70°N for composites (wEN − cEN) during Smin and Smax conditions for (a, b) WACCM3 and (c, d) ERA-40. Contours are drawn every 1 K. Dashed contours denote negative values. Significant anomalies computed through a Monte Carlo test (see text for more details) are shadowed in light (dark) gray for 90% (95%) significance levels.

anomalies in the zonal mean zonal wind as expected from thermal wind balance. Although the composites are not shown here, a weakening of the polar vortex, which moves downward in height with time, is simulated during Smin conditions. In contrast, during Smax, the winds strengthen in the polar stratosphere.

[14] To quantify the modulation of the downward propagation of the ENSO signal by the solar cycle, the temporal evolution of WACCM3 zonal mean temperature at 70°N is displayed in Figures 2a and 2b for wEN − cEN events, during Smin and Smax conditions. This diagnostic was first used by *Manzini et al.* [2006] to illustrate this behavior in the polar stratosphere in their model and observations. It has been widely used afterward when analyzing different aspects of the ENSO signal and its interactions with other sources of variability in models and observations [e.g., *Ineson and Scaife*, 2009; *Cagnazzo et al.*, 2009; *Cagnazzo and Manzini*, 2009; *Calvo et al.*, 2009]. Figures 2a and 2b highlight the findings already shown in Figure 1 at polar latitudes: during Smin, an anomalous warming in the polar region is simulated and it descends downward with time from December to March. During Smax, a stronger anomalous warming is located in the upper stratosphere while in the middle and lower stratosphere an anomalous cooling appears. Large differences between these two cases occur in the lower stratosphere and are significant at the 95% level from January to March according to a student *t* test.

[15] Analogous to Figures 2a and 2b, Figures 2c and 2d show results from ERA-40 reanalysis data. The downward propagation of the anomalous warming at polar latitudes is observed during Smin. Anomalous polar warming with the largest values at about 35 km in December descends to about 25 km in February, and reaches the lowermost stratosphere in March. During Smax, anomalous warming is observed in the middle and upper stratosphere from December to March in agreement with WACCM3 results, although only statistically significant in December. Contrary to WACCM3, no significant cooling is observed in the polar lower stratosphere during Smax; almost no ENSO signal is obtained there. Thus, the comparison of model and reanalysis anomalies at this and other polar latitudes reveals that overall, larger anomalies in ERA-40 are observed in Smin than in Smax conditions peaking one month earlier than in the model, although the patterns are quite similar, especially during Smin. The lag in the model response is probably related to the later winter to spring transition simulated by different versions of WACCM and reported in other studies [e.g., *SPARC CCMVal*, 2010, Figure 4.27). In addition, it is important to keep in mind that we do not expect the same response in both data sets. On one hand, additional sources of variability present in ERA-40 are

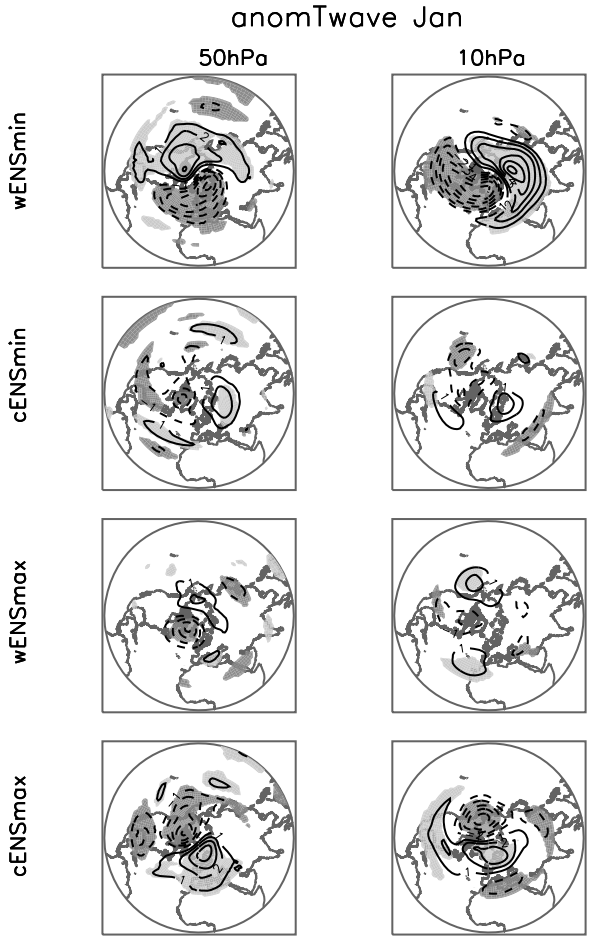


**Figure 3.** Detrended eddy temperature anomalies (computed as the full temperature field minus the zonal mean values) in January at 50 hPa and 10 hPa composited for wENSmin, cENSmin, wENSmax, and cENSmax. Contours are drawn every 1 K. Dashed contours denote negative values. Significant anomalies computed through a Monte Carlo test (see text for more details) are shadowed in light (dark) gray for positive (negative) values at 95% significance levels.

not included in these WACCM3 simulations, such as the volcanic aerosol heating and the QBO. To minimize their effects, a multiple linear regression has been performed to ERA-40 data (as in the work of *Calvo et al.* [2010] except that only the QBO and volcanic aerosols are used as predictors). However, this methodology cannot eliminate nonlinear effects between the QBO and ENSO or solar variability, which are known to occur as discussed in section 1. On the other hand, only one realization of the "real world" is available versus three different ones in WACCM. Therefore, it is reasonable that ERA-40 shows smaller regions of statistically significant changes in some cases. The comparison between the model and reanalysis does highlight the main differences in the polar ENSO signal between solar phases: an anomalous warming propagating downward throughout the winter from the upper to the lower stratosphere in Smin conditions while it is located in the upper stratosphere from December to March during Smax.

[16] The downward propagation of the ENSO shown in Figure 2 from early to late winter is the result of the interaction of the background flow and the planetary waves, which propagate upward toward the polar stratosphere during warm ENSO events [e.g., *Manzini et al.*, 2006]. As the waves dissipate, the background flow weakens and thus the area where subsequent waves dissipate and affect the background stratosphere appears at lower altitude. Figure 3 shows anomalies in the stationary eddy temperature field, computed as the total field minus the zonal mean field, for January at 50 and 10 hPa for wENSmin, wENSmax, cENSmin and cENSmax composites. Light and dark gray denotes 95% significant positive and negative anomalies, respectively. During wENSmin conditions (first row), the characteristic wave number 1 structure is clearly seen. The westward displacement of this pattern with height (compare the wavefield at 50 and 10 hPa) indicates upward wave propagation, which agrees with previous studies where the ENSO signal was analyzed in GCMs without considering solar cycle variability [*Sassi et al.*, 2004; *Manzini et al.*, 2006; *Garfinkel and Hartmann*, 2008]. In contrast, the wave signature observed in the stratosphere during Smax conditions is very weak during warm ENSO events (wENSmax). Little wave structure or upward wave propagation is noticeable, which indicates a fairly stationary state compared to Smin-wEN. For cold ENSOs, a weak wave train type pattern is observed at 50 hPa with almost no vertical propagation. During Smax (cENSmax), the wave pattern at 50 hPa is very similar to wENSmin conditions although with opposite phase. However, contrary to wENSmin, the signal does not propagate higher up (i.e., almost no westward displacement of the pattern when 50 and 10 hPa are compared) and it weakens at 10 hPa. Similar signals are obtained for other boreal winter months (not shown here).

[17] These results suggest that the intensified upward wave propagation observed during wENSmin conditions is inhibited during wENSmax, while during cold ENSO events, the upward propagation seems to be more effective during Smax than Smin conditions even though it never reaches as high as during wENSmin. These differences in wave patterns could be attributed to changes in wave generation in the troposphere between Smax and Smin phases or by a solar cycle modulation of the wave propagation and dissipation in the stratosphere linked to changes in the background flow. Both hypotheses are discussed next.

[18] First, the possible influence of SSTs on the tropospheric ENSO teleconnection patterns is investigated. *Kodera* [2005] found a positive correlation between the N34 index in July–August and the SSTs 6 months later (January–February) over the Indian Ocean. The correlation was stronger during Smin than Smax. We examined the observed SSTs used to drive the model and only found some differences between Smax and Smin composites over limited regions of the Indian Ocean during cold ENSO events. The typical cold anomalies observed during a La Niña event over the Indian Ocean were more intense during cENSmin than cENSmax. However, these differences were not statistically significant (not shown). This result does not contradict *Kodera* [2005] who found that the correlation held when the extreme ENSO events (those with N3.4 index exceeding $\pm 0.8$ standard deviation) were eliminated, suggesting that the differences

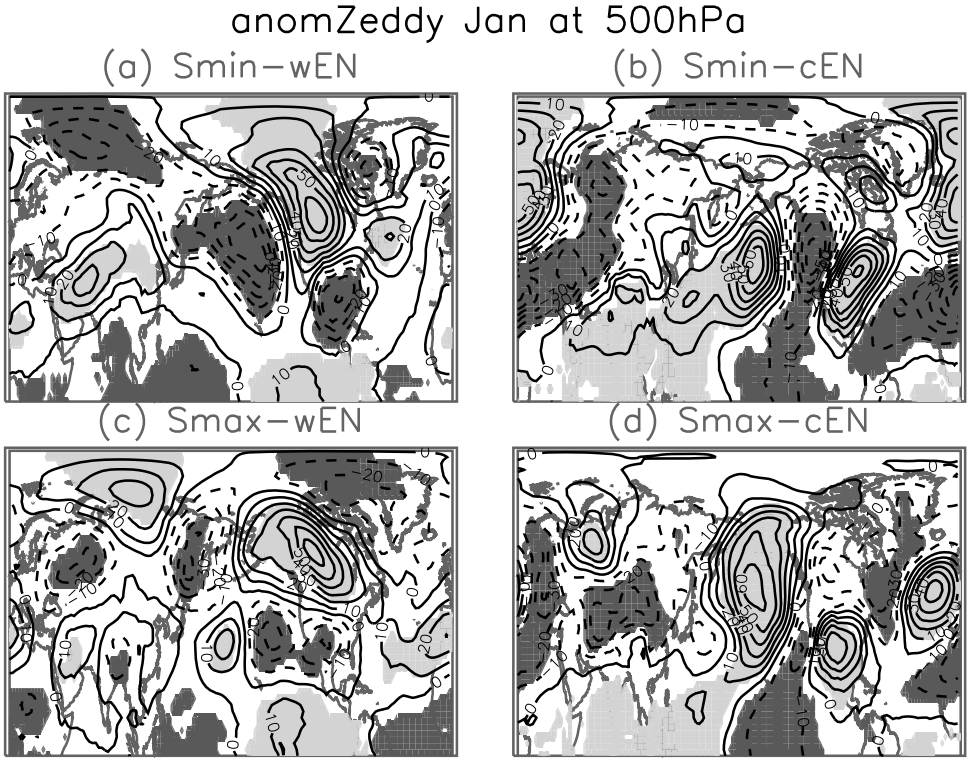


**Figure 4.** As in Figure 3 for eddy geopotential height anomalies at 500 hPa. Contours are drawn every 10 m.

between solar phases were related to SSTs variability and not necessarily to strong ENSO events. Since no significant solar signal in tropical SSTs is found during ENSO events, large differences in the tropospheric ENSO teleconnections in the NH middle latitudes in relation to SST changes are not expected in WACCM3. This is shown in Figure 4, which depicts eddy geopotential height at 500 hPa in January (other months show similar results). These panels show a PNA-like pattern characteristic of ENSO events, a negative center over the western Pacific, positive over the western part of North America and negative anomalies over the southernmost part of North America (the opposite during cEN). Moreover, the analysis of the amplitudes of the stationary wave number 1 derived from monthly mean temperatures anomalies at different levels shows differences between Smax and Smin conditions for wEN and cEN events at middle and high latitudes only in the stratosphere (Figure 5). There, the amplitude is the largest during wENSmin and the smallest during wENSmax. In the troposphere, little difference is observed between these cases. Overall, these results do not indicate large changes in wave generation in the troposphere and therefore, point to stratospheric changes in wave propagation and dissipation as the main mechanism to explain the differences in the polar stratosphere ENSO signal between solar maximum and solar minimum phases.

[19] As mentioned above, several studies have shown an anomalous warming in the tropical upper stratosphere during Smax compared with Smin conditions. These anomalies in temperature change the meridional temperature gradient and generate westerly anomalies in the zonal mean zonal wind field in the subtropics. This has been shown in both observations and models [*Kodera and Kuroda*, 2002; *Matthes et al.*, 2004; *Marsh et al.*, 2007]. For example, *Marsh et al.* [2007, Figures 14 and 15] show the annual mean response in temperature and zonal mean zonal wind under fixed Smax or Smin conditions in WACCM3 with no QBO and climatological SSTs. A similar figure for Smax − Smin differences from December to March is shown in Figure 6; no stratification according to ENSO events has been performed. Note that different from *Marsh et al.* [2007] and *Matthes et al.* [2004], observed SSTs are used as boundary conditions in our simulations. The solar signal response in the extratropics appears in WACCM3 as a significant warming in the upper stratosphere in boreal winter months and a smaller cooling below. Significant westerly anomalies are observed in the subtropics in January in the upper stratosphere, moving downward and poleward throughout the winter in agreement with the mechanism proposed by *Kodera and Kuroda* [2002]. These anomalies in the background wind can affect the propagation of planetary waves simulated during ENSO events, and consequently, modulate the ENSO signal in the polar stratosphere.

[20] We calculated wave index of refraction [*Matsuno*, 1970] for each of the four composites analyzed here, following the methodology explained by *Calvo and Garcia* [2009]. The largest differences occur during warm ENSO events in wave number 1 between Smax and Smin conditions. Figure 7 shows squared index of refraction for k = 1 wave component for wENSmin and wENSmax in January. During warm ENSO events, larger index of refraction values are present throughout the stratosphere between 70°N and 80°N during Smin compared to Smax conditions, favoring wave propagation during wENSmin. This behavior is noticeable in December, maximizes in January and

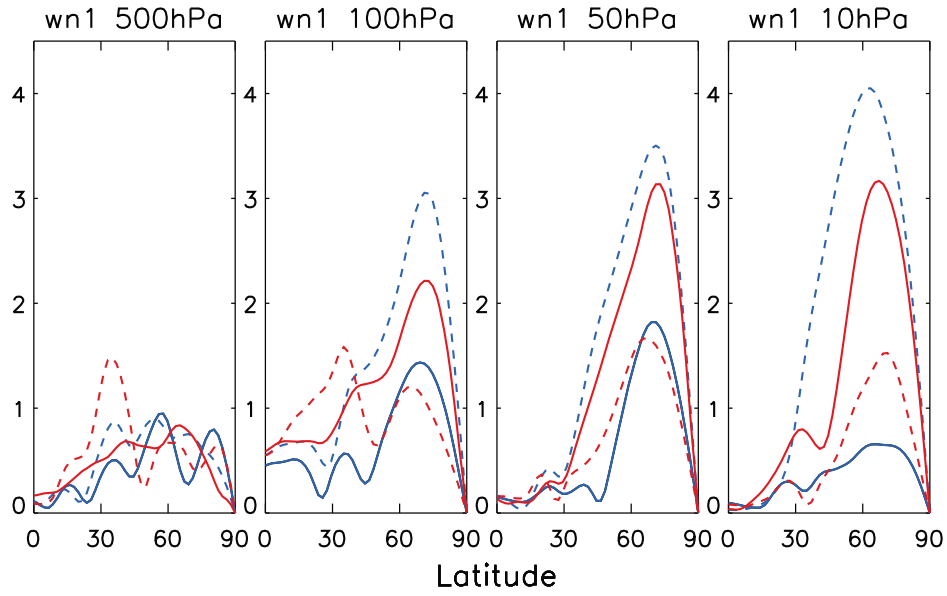


**Figure 5.** Composites of wave number 1 temperature amplitude anomalies (K) for January at 500 hPa, 100 hPa, 50 hPa and 10 hPa for wENSmax (blue solid lines), wENSmin (blue dashed lines), cENSmax (red solid lines), and cENSmin (red dashed lines).

February and is small in March. In addition, during wENSmax, a larger gradient in the index of refraction is simulated in the subtropics between 20 and 30 km, favoring equatorward propagation.

[21] Superimposed on the wave index of refraction in Figure 7 are Eliassen-Palm (EP) flux vectors. The EP flux is a measure of wave propagation from one latitude and altitude to another [*Edmon et al.*, 1980]. EP fluxes are calculated from the full dynamical field (i.e., no wave number selection)

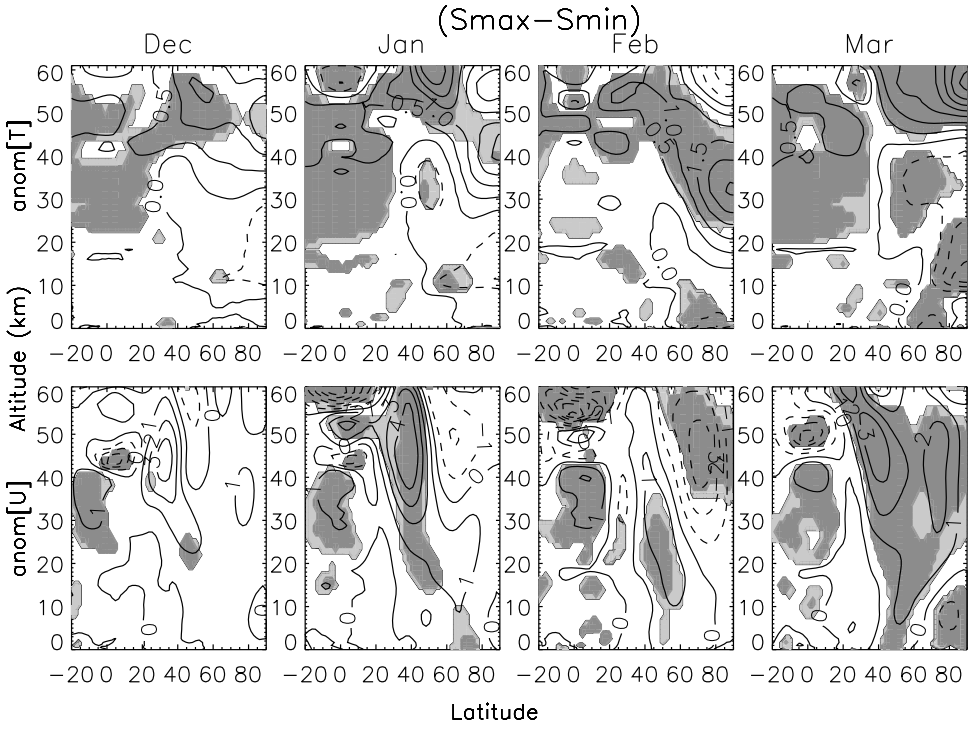


**Figure 6.** Smax − Smin composites of the detrended (top) zonal mean temperature and (bottom) zonal wind anomalies. Contours are drawn every 0.5 K for temperature and 1 m $s^{-1}$ for zonal wind. Dashed contours denote negative differences. Significant anomalies computed through a Monte Carlo test (see text for more details) are shadowed in light (dark) gray for 90% (95%) significance levels. Vertical coordinate is log-pressure altitude.

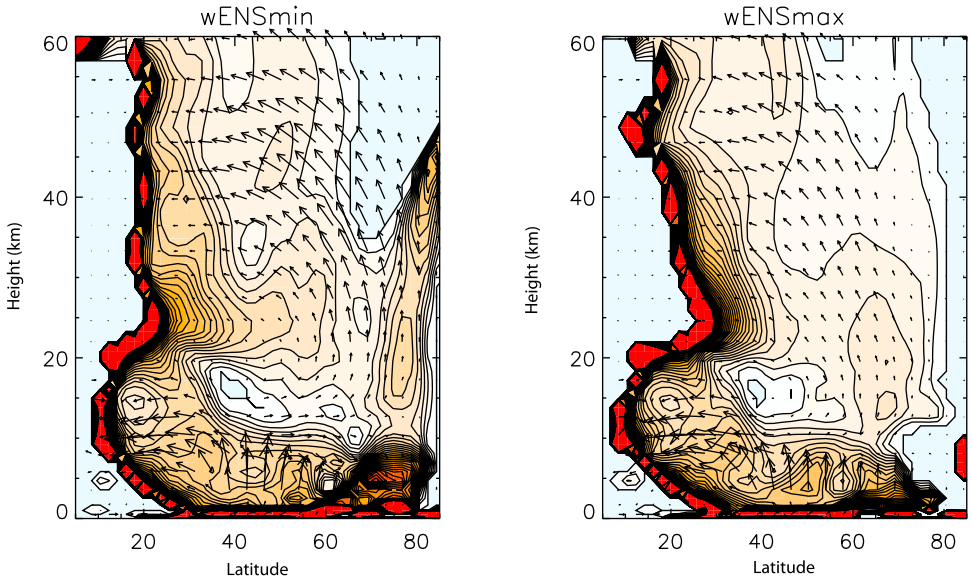


**Figure 7.** Cross section (latitude versus log-pressure altitude) of the wave index of refraction squared for k = 1 wave component (contours) and EP flux (arrows) for the composites (left) wENSmin and (right) wENSmax in January. Contours are drawn every 10 units. The EP fluxes account for the aspect ratio such as Fy/Fz $\sim$ 100. They are scaled by a factor $e^{z/10}$ to account for the decrease of density with height.

at each time step of the model and average together to obtain monthly mean values. Both Smin and Smax cases show upward and equatorward propagation in the stratosphere. While in Smin the upward propagation extends toward high altitudes, this does not occur during Smax, in agreement with the differences simulated in refractive index in this region. In addition, the magnitude of the EP flux is larger in the middle to high latitudes in the middle and upper stratosphere during Smin. In the troposphere no clear differences are simulated: upward propagation of waves occurs at middle latitudes (between 40°N and 60°N) in both wENSmin and wENSmax. Most waves are then refracted toward the subtropics. The remaining waves propagate upward into the stratosphere in both cases. Strong poleward wave activity occurs in wENSmin in the transition region between troposphere and stratosphere allowing for upward propagation in the polar stratosphere following regions of large index of refraction. In wENSmax the upward propagation in the stratosphere is present mainly at middle latitudes. During cEN events (not shown), larger wave number 1 index of refraction values occur in the middle latitudes (40°N–60°N) in the lower stratosphere during cENSmax and in the subtropical troposphere during cENSmin. As a result, stronger upward wave activity in the stratosphere at middle latitudes occurs during cENSmax compared to cENSmin. No upward propagation at polar latitudes is observed in any cold ENSO case.

[22] Finally, to illustrate the seasonal evolution and quantify the differences in wave mean flow interactions between solar phases, Figure 8 shows the vertical profile of the composite differences wEN − cEN for the horizontal and vertical EP flux components (Fy and Fz) and its divergence (divEP) during Smin and Smax conditions. Fy and Fz have been averaged between 60°N and 80°N and divEP between 50°N to 80°N. A wider latitude range in the EP flux divergence has been chosen as waves generally propagate upward and equatorward so that the largest dissipation area occurs slightly equatorward from the region of largest propagation. In any case, similar EP flux profiles are obtained when the 50°N–80°N latitude range is considered for Fz and Fy.

[23] During Smin conditions, Fz composites (Figure 8a) show upward propagation for ENSO events (wEN − cEN composites) throughout the winter. This is mainly due to the anomalous increase of upward propagation during wEN events while the cEN events have little effect on the vertical component of the EP flux (not shown). The meridional component Fy (Figure 8c) shows poleward propagation for wEN − cEN composites and Smin conditions below 25 km during January and February. This is the result of both anomalous equatorward propagation during cEN events and poleward propagation during wEN events (not shown). In March, the upward propagation becomes equatorward (negative values of Fy). In terms of EP flux divergence (Figure 8e), the entire winter shows anomalous wEN − cEN convergence in the upper stratosphere, again mainly due to the effect of wEN events. Overall, these results during Smin are in agreement with previous analysis of the ENSO signal when it operates independently of other sources of variability [*García-Herrera et al.*, 2006].

[24] During Smax (Figures 8b, 8d, and 8f), wEN − cEN composites show anomalous downwelling (less upward propagation than the climatology, negative Fz values) in January and February together with anomalous equatorward propagation below 30 km (negative Fy anomalies) and positive anomalous EP flux divergence; as expected from the intensification of the westerly winds in the subtropics during Smax compared to Smin conditions (Figure 6). Only March shows anomalous upward propagation in the lower polar stratosphere with a stronger equatorward component and little anomalous dissipation (anomalous convergence) in the upper stratosphere. As in Smin, this behavior in the wEN − cEN differences is dominated by the warm ENSO events (not shown) when the largest differences with respect to the

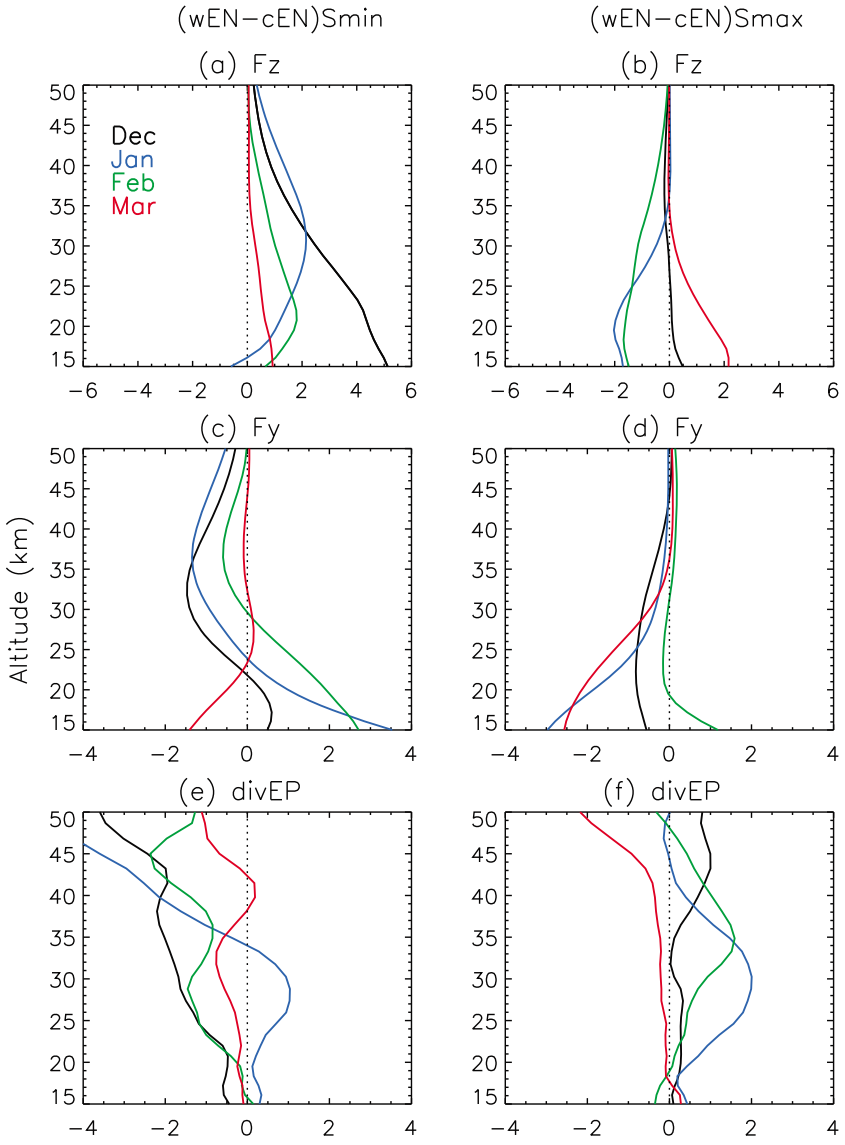


**Figure 8.** Vertical profiles for the wEN − cEN composite differences during (a, c, e) Smin conditions and (b, d, f) Smax conditions of the (top) vertical and (middle) meridional components of the Eliassen-Palm flux averaged from 60°N to 80°N and the Eliassen-Palm flux divergence (bottom) averaged from 50°N to 80°N. Values are area weighted. Plotted values are $10^6$Fy, $10^4$Fz in kg $s^{-2}$ and in m $s^{-1}$ $d^{-1}$ for EP flux divergence. Solid lines for winter months: December (black), January (blue), February (green), and March (red).

monthly mean climatology occur at high latitudes: more equatorward propagation and less upward propagation.

[25] It is clear from the above analysis that anomalies in the background winds generated during solar maximum conditions in tropical temperature can modulate the enhanced propagation of planetary waves at middle latitudes simulated during warm ENSO events, favoring a more equatorward propagation of the waves and thus, making the polar vortex more stable during Smax.

### 3.2. ENSO Impact on the 11 Year Solar Cycle Signal

[26] The 11 year solar signal in the Northern Hemisphere is presented in Figure 6 for zonal mean temperature and zonal wind. Despite the general agreement with the solar signal obtained from reanalysis data [*Kodera and Kuroda*, 2002; *Matthes et al.*, 2004] as discussed above, several differences are noted. The stronger westerly winds simulated in Smax − Smin in the subtropics in December and January do not reach polar latitudes in the upper stratosphere as they do in the reanalysis. The anomalous cooling simulated in the polar lower stratatosphere is not as intense, but similar to other model results, as FUB-CMAM [see *Matthes et al.*, 2004, Figure 4a]. Finally, the solar signal in March largely differs from observations [*Matthes et al.*, 2004; *Gray et al.*, 2004]. *Matthes et al.* [2004] suggested that a good model climatology is a requirement to reproduce a realistic solar signal. The climatological winds in WACCM3 and its variability have been compared to ERA-40 climatology in Figure 9. Overall, the model winds at midlatitudes and high latitudes in the middle stratosphere are weaker in December and become consistently too strong from January to March. This is also related to the too low frequency of major warmings in this

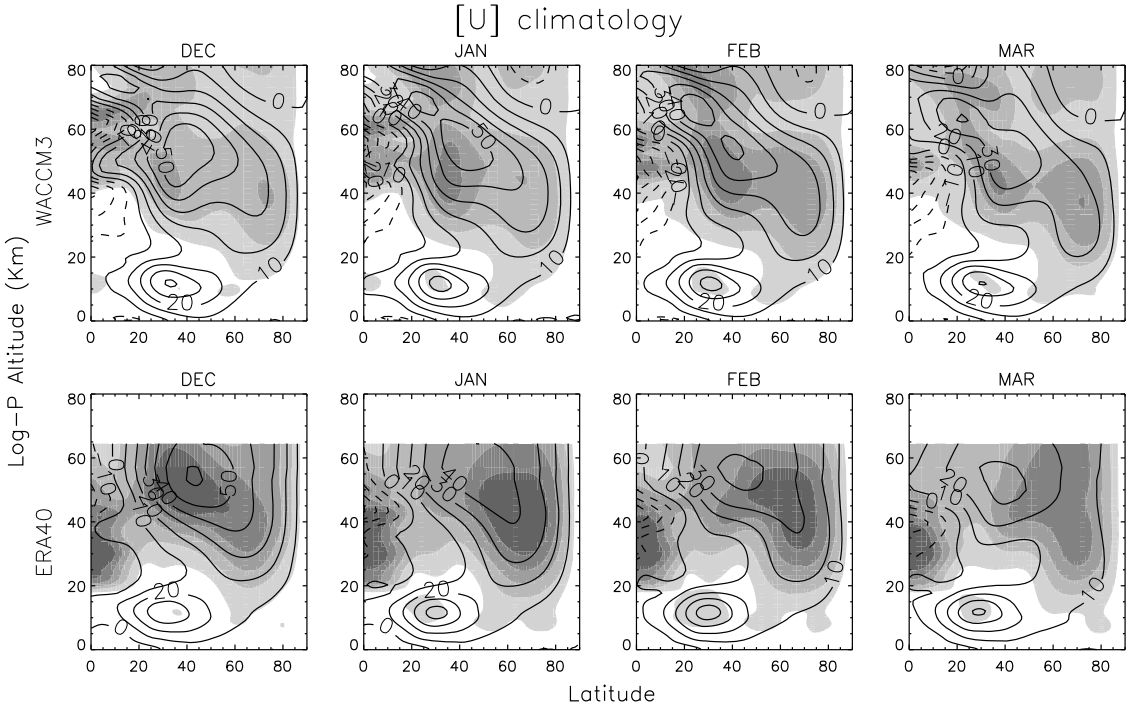


**Figure 9.** Monthly mean climatology from December to March for the ensemble mean of the (top) three WACCM3 simulations and (bottom) ERA-40 reanalysis. Solid (dashed) lines are for westerly (easterly) winds. Contours are drawn every 10 m $s^{-1}$. Vertical coordinate is log-pressure altitude.

model compared to observations, as discussed by *Richter et al.* [2010]. Further evidence can be seen in Figure 9, which shows lower values in the standard deviation and therefore lower polar variability. In the upper stratosphere and lower mesosphere the main difference is the fact that the jet in the model does not reach polar latitudes as observed in the reanalysis. This could explain the lack of poleward displacement of the solar signal toward high latitudes and the weaker anomalous cooling in the polar lower stratosphere (Figure 6). Interestingly, when the Smax − Smin composites are computed for neutral ENSO events, the solar signal in March looks more similar to that from the reanalysis record. With these considerations in mind, we analyze next the impact of ENSO on the extratropical solar signal by comparing Smax − Smin composites during cEN and wEN events.

[27] Figures 10 and 11 show Smax − Smin composite differences in zonal mean temperature and zonal mean zonal wind for wEN and cEN events. During cEN (Figures 10 (top) and 11 (top)), an anomalous warming and weaker winds are observed in the polar region from December to February. These signals descend with height from the stratopause in December to the lower stratosphere in February. Anomalies of opposite sign are observed above them in the upper stratosphere and lower mesosphere and descend to the middle polar stratosphere in March. These signals are similar to those obtained when no stratification with respect to the phase of ENSO was performed (Figure 6), although the values are larger. Nevertheless, in both cEN conditions and when no stratification according to the ENSO phase is performed (Figure 6), the solar signal in the polar regions in the stratosphere is only significant in February and March. In the case of warm ENSO events (Figures 10 (bottom) and 11 (bottom)) the Smax − Smin signal shows quite a different pattern. Significant cold anomalies are observed in the polar lower stratosphere with warmer temperatures in the upper stratosphere lower mesosphere, which are accompanied by a stronger polar vortex. Contrary to cEN conditions, the location of the polar anomalies does not change with time throughout the winter.

[28] These results concur with those from *Hampson et al.* [2005] who studied the role of planetary wave forcing on the effect of the 11 year solar cycle in the polar stratosphere. In their mechanistic model, they obtain a Smax − Smin signal with warming in the lower stratosphere and cooling in the lower mesosphere in February and March when the planetary wave forcing is weak. This is similar to the solar response obtained during cold ENSO conditions (Figure 10, top). Under strong planetary wave forcing, the polar Smax − Smin signal is reversed and stronger. This change in response agrees well with the Smax − Smin signal obtained in Figure 10 (bottom), since warm ENSO events are also associated to large planetary wave amplitude.

[29] In WACCM3, the different behavior of the solar signal during warm ENSO events is characterized by a cooling in the lowermost stratosphere, which is not observed during cEN or when no stratification according to the ENSO phase is performed (Figure 6). These differences arise mainly from the anomalous cooling simulated during wENSmax (not shown). As in the analysis of the ENSO signal, when both Smax and warm ENSO conditions coincide, the wave mean flow interaction at high latitudes, observed during warm ENSO events, is inhibited and the extratropical stratosphere is no longer perturbed. The EP fluxes and their divergences shown in Figure 12 for Smax − Smin composites corroborate this mechanism. During cEN events the Smax − Smin signal

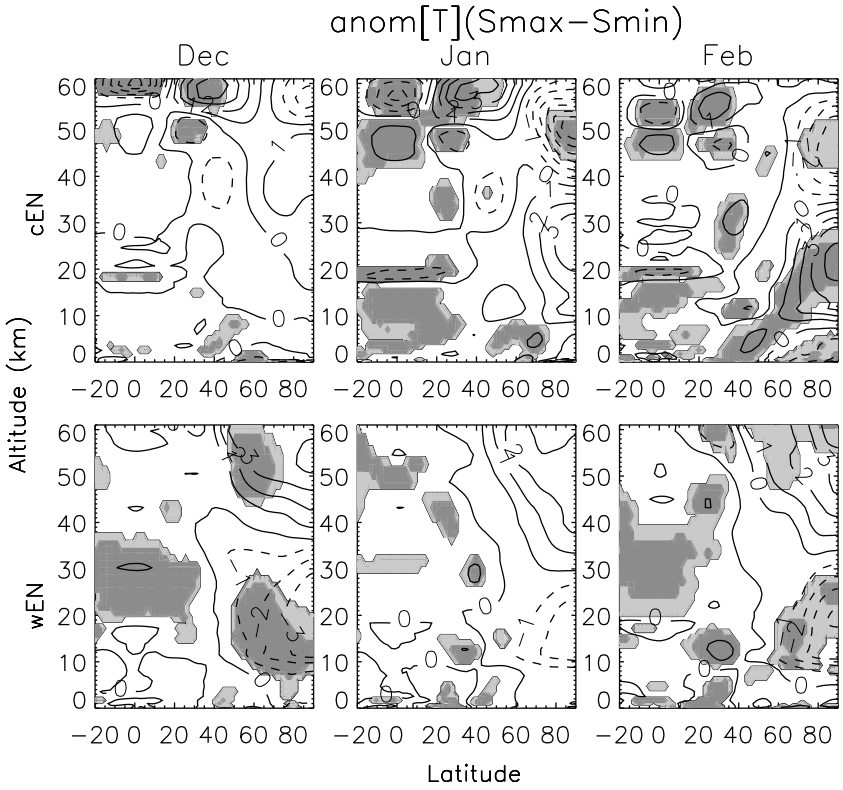


**Figure 10.** Same as in Figure 1 but for the composite differences (top) Smax − Smin cEN conditions and (bottom) Smax − Smin wEN conditions.

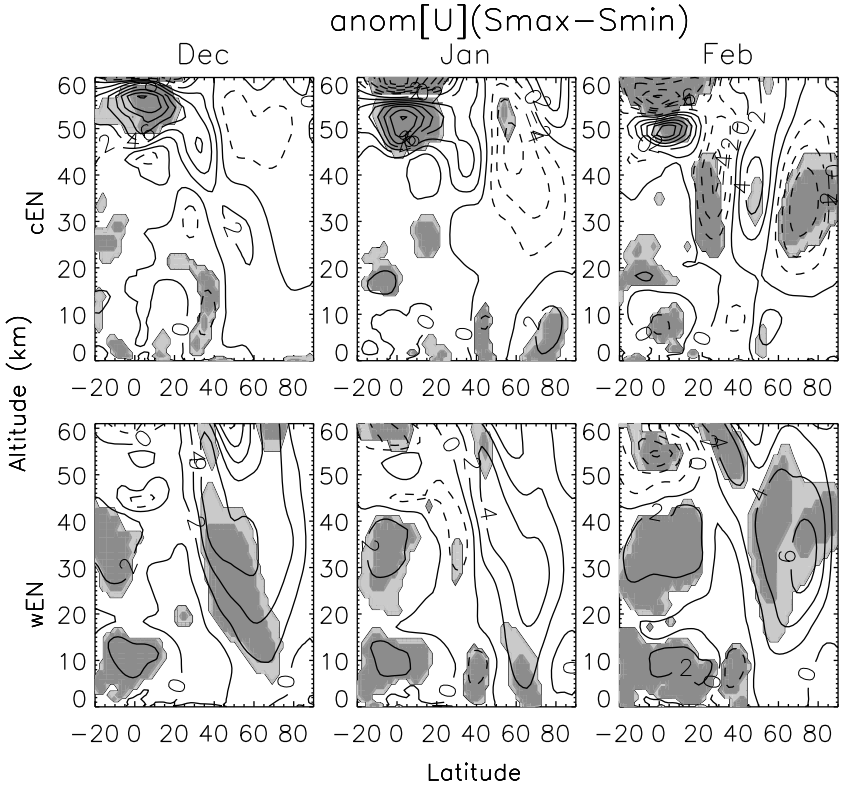


**Figure 11.** Same as in Figure 10 but for zonal mean zonal wind. Contours are drawn every 1 m $s^{-1}$.

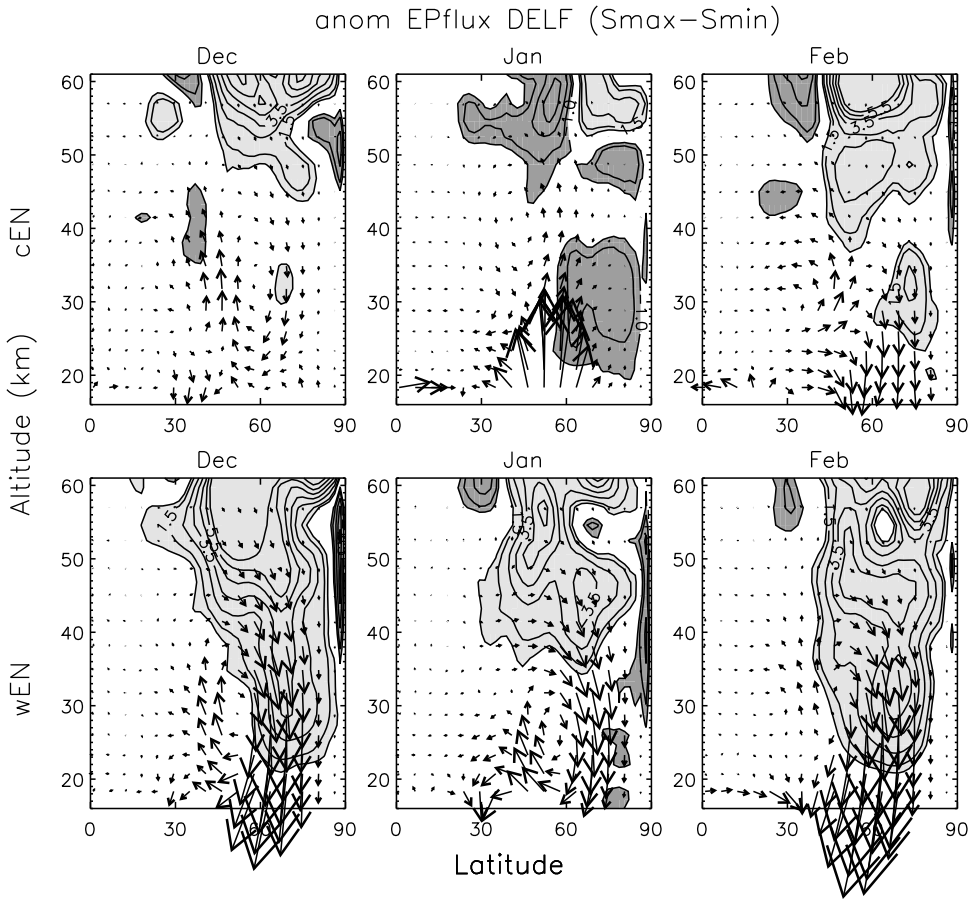


**Figure 12.** Same as in Figure 10 but for anomalies in EP flux (arrows) and its divergence (contours). Values plotted are Fy $\times$ $10^6$, Fz $\times$ 2.5 $\times$ $10^4$ in kg $s^{-2}$. Contours for EP flux divergence are drawn at $\pm$0.5, 1, 1.5, 2.5, 3.5, 4.5 $m^{-1}$ $s^{-1}$ $d^{-1}$. Light (dark) gray for positive (negative) EP flux divergence. Fz, Fy are latitude weighted multiplied by cos (lat).

in the EP flux and its divergence at high latitudes is small. At middle latitudes, some upward propagation is observed from December to February mainly due to the anomalous upward propagation during cEN − Smax (not shown). In contrast, the behavior during wEN events seems to be much more robust throughout the winter. Downward wave propagation anomalies (negative values of Fz anomalies) compared to the climatology are obtained, accompanied by equatorward and upward anomalies in the subtropics. In terms of the EP flux divergence, much larger positive anomalies are simulated during wEN events. Therefore, less upward and more equatorward wave propagation is observed in Smax − Smin differences during warm ENSO at mid and high latitudes, which increases the strength of the polar vortex and makes it colder as shown in Figures 10 and 11.

[30] In terms of the conceptual framework first proposed by *Kodera and Kuroda* [2002] to explain the solar signal at polar latitudes, the modulation of the solar signal by ENSO can be understood as follows: wEN events reinforce the positive anomalies in the polar night jet and intensifies them at polar latitudes, anomalous downward wave propagation is simulated at polar latitudes. This suggests a longer radiative state with a delayed transition to the dynamical state in late winter despite warm ENSO events are characterized by a stronger upward propagation at polar latitudes. This result highlights the nonadditive response of ENSO and solar forcings. On the contrary, during cEN events, the polar stratosphere warms earlier, favoring an earlier onset of the dynamical phase.

## 4. Summary and Discussion

[31] Three transient simulations (1950–2004) from WACCM have been analyzed to investigate the effects of changes in solar irradiance over the 11 year solar cycle on the ENSO signal in the boreal winter polar stratosphere and, in turn, the impact of ENSO on the NH extratropical 11 year solar cycle signal in winter. These simulations do not include a QBO, neither internally generated nor prescribed from observations, or stratospheric heating from volcanic aerosols.

[32] During solar minimum conditions the NH polar stratosphere responds to ENSO in the same way as reported in previous studies; that is, warm events lead to a weaker polar vortex and a warmer polar stratosphere compared to cold events. A downward propagation of the ENSO signal throughout the winter, due to anomalous wave propagation and dissipation, is simulated during Smin conditions. However, during solar maximum, little downward propagation is observed at high latitudes. These results are also reproduced in ERA-40 reanalysis. Warmer temperatures are observed in

the upper stratosphere and colder temperatures in the lower stratosphere (below 30 km) in WACCM3 simulations during Smax accompanied by a stronger polar vortex. We have shown that this different behavior is mainly due to the state of the atmosphere during wENSmax conditions. In this case, the upward propagation of ultralong Rossby waves, mainly wave number 1, toward high latitudes, characteristic of wEN-Smin events, is inhibited and, instead, a more equatorward propagation is observed. This is the result of the direct 11 year solar cycle signal in the tropical upper stratosphere (a warming during Smax compared to Smin) and not to a direct influence of the solar influence on the SSTs. This modulation in temperature changes the background winds in the subtropics and favors wave propagation toward those latitudes, leading to a less disturbed polar region.

[33] The effects of ENSO on the extratropical 11 year solar cycle signal in boreal winter were also investigated. Without stratifying by the phase of ENSO, a strengthening of the westerlies in the subtropics, which moves poleward and downward as the winter evolves, is observed in Smax compared to Smin conditions. In the polar regions, the 11 year solar signal appears as weaker winds in the upper stratosphere and an anomalous warming is observed in this region mainly in January and February in agreement with results from *Matthes et al.* [2004]. When the solar signal is stratified according to ENSO, the pattern at high latitudes is similar during cEN events although it is important to note that the anomalies in the polar stratosphere are only significant in February and March in both cases, which could be related to deficiencies in the model zonal mean zonal wind climatology. During warm ENSO events, the warmer polar anomalies are simulated at higher levels in the upper stratosphere, while the polar lower stratosphere is anomalously cold and the polar vortex strengthens. The anomalies and significant regions are larger than in the cEN case throughout the winter. In addition, no downward propagation of the solar signal is observed during wEN conditions. As in the case of the ENSO signal, we have shown that this is mainly due to the anomalous wave mean flow interaction during Smax − wEN conditions.

[34] In our simulations it appears that when both warm ENSO events and Smax conditions coincide, the net effect in winter is not to increase the level of perturbation of the polar stratosphere, as it would be if both forcings operated independently, but to inhibit the planetary wave activity toward high latitudes to such an extent that the lower polar stratosphere becomes colder and the polar vortex stronger. This reveals the nonlinear response of the polar stratosphere to ENSO/solar interactions.

[35] *Kuroda* [2007] and *Kryjov and Park* [2007] analyzed the ENSO modulation of the solar cycle signal on the NAO and the solar signal modulation of ENSO on the NAM, respectively, using ERA-40 and NCEP/NCAR reanalysis data. As in our study, they both showed a nonlinear behavior in the response. This highlights the need to take into account the phases of both of these phenomena when studying their effects on the polar stratosphere. However, some differences between their results and ours are noticeable. *Kuroda* [2007] found a weaker solar cycle modulation of the NAO in the warm phase of ENSO compared to the cold phase. *Kryjov and Park* [2007] found null ENSO response in the stratosphere at high latitudes during Smax compared to Smin. One of the factors responsible for the discrepancy between these studies and our results might be the influence of the QBO in the solar/ENSO interaction. The fact that both studies did not account for strong ENSO events (stronger than for instance one standard deviation) but analyzed the stratospheric response to SSTs might also play a role. Another aspect to consider is that these previous studies show the winter average (DJF), while we have analyzed the winter seasonal march. We have shown here the need to analyze the seasonal evolution of the downward propagation, since a winter average might cancel signals of different origins that might be located at the same height in different months. For instance, in our study, the solar signals in January or February might seem opposite to each other during wEN and cEN conditions when no temporal evolution is considered (Figures 10 and 11). However, when the seasonal march is analyzed, it is clear that the signal does not reverse. Instead, changes in the wave mean flow interaction move the location of the response.

[36] It is important to note that the solar signal obtained in our study in February during cEN and wEN events resembles that obtained in a different WACCM simulation, which used climatological SSTs (i.e., no ENSO variability) but included a QBO (K. Matthes, personnal communication, 2010). It also agrees with results from *Gray et al.* [2004, Figure 13] (e.g., February months) when ERA-40 data is stratified according to the QBO phase. In both cEN and QBO west phases (the less perturbed states), the solar signal (Smax − Smin) appears as a warm anomaly in the polar lower stratosphere with cooling above and therefore a weaker polar vortex. In the case of wEN or QBO east phase, the solar signal in the polar stratosphere shows cooling in its lowermost part of the polar stratosphere and warming above, and strengthened zonal mean zonal winds. Since the solar signal appears in both interactions with ENSO and QBO, it seems reasonable to think that this is a robust feature of the polar variability. In addition, studies of the ENSO/QBO interactions show weaker ENSO or QBO signals and changes with time in the response when these phenomena coincide with easterly QBO phase or warm ENSO events (the most perturbed phases in each case) [*Wei et al.*, 2007; *Garfinkel and Hartmann*, 2007; *Calvo et al.*, 2009]. Therefore, despite there being still some controversy in quantifying the response, all these studies point toward a general conclusion: whenever a combination of two external forcing ENSO, QBO or solar variability, which act to perturb the polar stratosphere operates simultaneously, they do not produce an additive response as expected when they operate independently.

[37] We note in closing that we have used three ensemble members in this study to analyze the combined response of two different forcings in the polar stratosphere. In contrast, in the real world, studying the variability at high latitudes requires the analysis of at least three factors (ENSO, QBO, 11 year solar cycle) in one single realization. Therefore, over a short period of time (about 30 years for the satellite era) it is quite unlikely to be able to separate all these three factors to fully understand the nonlinear interactions among them and their combined response in the polar stratosphere.

[38] **Acknowledgments.** The authors want to thank Rolando R. Garcia, Isabel Zubiaurre, and Gabiel Chiodo for useful discussions on wave mean flow interaction and index of refraction diagnostics, sea surface temperatures, and solar signal, respectively. We also acknowledge

the three reviewers for their constructive comments and suggestions. N. Calvo was supported by the Spanish Ministry of Education and Science and the Fulbright Commission in Spain and by the Advanced Study Programme from the National Center for Atmospheric Research (ASP-NCAR). The WACCM simulations were carried out at the NASA Advanced Supercomputing Division (NAS) in Ames, CA; and at the Barcelona Supercomputing Center (BSC) in Barcelona, Spain. The use of these computational facilities is gratefully acknowledged. NCAR is sponsored by the U.S. National Science Foundation.

## References

Baldwin, M. P., et al. (2001), The quasi-biennial oscillation, *Rev. Geophys.*, *39*(2), 179–229, doi:10.1029/1999RG000073.

Cagnazzo, C., and E. Manzini (2009), Impact of the stratosphere on the winter tropospheric teleconnections between ENSO and the North Atlantic and European region, *J. Clim.*, *22*, 1223–1238, doi:10.1175/2008JCLI2549.1.

Cagnazzo, C., et al. (2009), Northern winter stratospheric temperature and ozone responses to ENSO inferred from an ensemble of chemistry climate models, *Atmos. Chem. Phys.*, *9*, 8935–8948, doi:10.5194/acp-9-8935-2009.

Calvo, N., and R. R. Garcia (2009), Wave forcing of the tropical upwelling in the lower stratosphere under increasing concentrations of greenhouse gases, *J. Atmos. Sci.*, *66*, 3184–3196, doi:10.1175/2009JAS3085.1.

Calvo, N., M. A. Giorgetta, and C. Peña-Ortiz (2007), Sensitivity of the boreal winter circulation in the middle atmosphere to the quasi-biennial oscillation in MAECHAM5 simulations, *J. Geophys. Res.*, *112*, D10124, doi:10.1029/2006JD007844.

Calvo, N., R. García-Herrera, and R. R. Garcia (2008), The ENSO signal in the stratosphere, in *Trends and Directions in Climate Research*, *Ann. N. Y. Acad. Sci.*, *1146*, 16–31, doi:10.1196/annals.1446.008.

Calvo, N., M. A. Giorgetta, R. García-Herrera, and E. Manzini (2009), Nonlinearity of the combined warm ENSO and QBO effects on the Northern Hemisphere polar vortex in MAECHAM5 simulations, *J. Geophys. Res.*, *114*, D13109, doi:10.1029/2008JD011445.

Calvo, N., R. R. Garcia, W. J. Randel, and D. R. Marsh (2010), Dynamical mechanism for increase in tropical upwelling in the lowermost tropical stratosphere during warm ENSO events, *J. Atmos. Sci.*, *67*, doi:10.1175/2010JAS3433.1.

Camp, C. D., and K.-K. Tung (2007), Stratospheric polar warming by ENSO in winter: A statistical study, *Geophys. Res. Lett.*, *34*, L04809, doi:10.1029/2006GL028521.

Collins, W. D., et al. (2004), Description of the NCAR Community Atmosphere Model (CAM3), *Tech. Rep., NCAR/TN-464 STR*, 266 pp., Natl. Cent. for Atmos. Res., Boulder, Colo.

Edmon, H. J., Jr., B. J. Hoskins, and M. E. McIntyre (1980), Eliassen-Palm cross sections for the troposphere, *J. Atmos. Sci.*, *37*, 2600–2616, doi:10.1175/1520-0469(1980)037<2600:EPCSFT>2.0.CO;2.

Free, M., and D. J. Seidel (2009), The observed temperature El Niño–Southern Oscillation temperature signal in the stratosphere, *J. Geophys. Res.*, *114*, D23108, doi:10.1029/2009JD012420.

Garcia, R. R., D. R. Marsh, D. E. Kinnison, B. A. Boville, and F. Sassi (2007), Simulation of secular trends in the middle atmosphere, 1950–2003, *J. Geophys. Res.*, *112*, D09301, doi:10.1029/2006JD007485.

García-Herrera, R., N. Calvo, R. R. Garcia, and M. A. Giorgetta (2006), Propagation of ENSO temperature signals into the middle atmosphere: A comparison of two general circulation models and ERA-40 reanalysis data, *J. Geophys. Res.*, *111*, D06101, doi:10.1029/2005JD006061.

Garfinkel, C. I., and D. L. Hartmann (2007), Effects of El Niño–Southern Oscillation and the quasi-biennial oscillation on polar temperatures in the stratosphere, *J. Geophys. Res.*, *112*, D19112, doi:10.1029/2007JD008481.

Garfinkel, C. I., and D. L. Hartmann (2008), Different ENSO teleconnections and their effects on the stratosphere polar vortex, *J. Geophys. Res.*, *113*, D18114, doi:10.1029/2008JD009920.

Gray, L. J., S. J. Phipps, T. J. Dunkerton, M. P. Baldwin, E. F. Drysdale, and M. R. Allen (2001), A data study of the influence of the equatorial upper stratosphere on Northern Hemisphere stratospheric sudden warmings, *Q. J. R. Meteorol. Soc.*, *127*, 1985–2003.

Gray, L. J., S. Crooks, C. Pascoe, S. Sparrow, and M. Palmer (2004), Solar and QBO influences on the timing of stratospheric sudden warmings, *J. Atmos. Sci.*, *61*, 2777–2796, doi:10.1175/JAS-3297.1.

Hamilton, K. (1993), An examination of observed Southern Oscillation effects in the Northern Hemisphere stratosphere, *J. Atmos. Sci.*, *50*, 3468–3474, doi:10.1175/1520-0469(1993)050<3468:AEOOSO>2.0.CO;2.

Hampson, J., P. Keckhut, A. Hauchecorne, and M. L. Chanin (2005), The effect of the 11-year solar-cycle on the temperature in the upper-stratosphere and mesosphere: Part II. Numerical simulations and the role of planetary waves, *J. Atmos. Sol. Terr. Phys.*, *67*, 948–958, doi:10.1016/j.jastp.2005.03.005.

Holton, J. R., and H.-C. Tan (1980), The influence of the equatorial quasi-biennial oscillation on the global circulation at 50 mb, *J. Atmos. Sci.*, *37*, 2200–2208, doi:10.1175/1520-0469(1980)037<2200:TIOTEQ>2.0.CO;2.

Holton, J. R., and H.-C. Tan (1982), The quasi-biennial oscillation in the Northern Hemisphere lower stratosphere, *J. Meteorol. Soc. Jpn.*, *60*, 140–148.

Hood, L. L. (2004), Effects of solar UV variability on the stratosphere, in *Solar Variability and Its Effects on Climate*, *Geophys. Monogr. Ser.*, vol. 141, edited by J. M. Pap and P. Fox, pp. 283–303, AGU, Washington, D. C., doi:10.1029/141GM20.

Ineson, S., and A. A. Scaife (2009), The role of the stratosphere in the European climate response to El Niño, *Nat. Geosci.*, *2*, 32–36, doi:10.1038/ngeo381.

Kodera, K. (2005), Possible solar modulation of the ENSO cycle, *Pap. Meteorol. Geophys.*, *55*, 21–32, doi:10.2467/mripapers.55.21.

Kodera, K., and Y. Kuroda (2002), Dynamical response to the solar cycle, *J. Geophys. Res.*, *107*(D24), 4749, doi:10.1029/2002JD002224.

Kryjov, V. N., and C.-K. Park (2007), Solar modulation of the El Niño/Southern Oscillation impact on the Northern Hemisphere annular mode, *Geophys. Res. Lett.*, *34*, L10701, doi:10.1029/2006GL028015.

Kuroda, Y. (2007), Effect of QBO and ENSO on the solar cycle modulation of winter North Atlantic oscillation, *J. Meteorol. Soc. Jpn.*, *85*, 889–898, doi:10.2151/jmsj.85.889.

Labitzke, K., and H. van Loon (1988), Associations between the 11-year solar cycle, the QBO and the atmosphere: Part I. The troposphere and stratosphere in the Northern Hemisphere winter, *J. Atmos. Terr. Phys.*, *50*, 197–206, doi:10.1016/0021-9169(88)90068-2.

Manzini, E., M. A. Giorgetta, M. Esch, L. Kornblueh, and E. Roeckner (2006), The influence of sea surface temperatures on the northern winter stratosphere: Ensemble simulations with the MAECHAM5 model, *J. Clim.*, *19*, 3863–3881, doi:10.1175/JCLI3826.1.

Marsh, D. R., R. R. Garcia, D. E. Kinnison, B. A. Boville, F. Sassi, S. C. Solomon, and K. Matthes (2007), Modeling the whole atmosphere response to solar cycle changes in radiative and geomagnetic forcing, *J. Geophys. Res.*, *112*, D23306, doi:10.1029/2006JD008306.

Matsuno, T. (1970), Vertical propagation of stationary planetary waves in the winter Northern Hemisphere, *J. Atmos. Sci.*, *27*, 871–883, doi:10.1175/1520-0469(1970)027<0871:VPOSPW>2.0.CO;2.

Matthes, K., U. Langematz, L. L. Gray, K. Kodera, and K. Labitzke (2004), Improved 11-year solar signal in the Freie Universität Berlin Climate Middle Atmosphere Model (FUB-CMAM), *J. Geophys. Res.*, *109*, D06101, doi:10.1029/2003JD004012.

Randel, W. J., R. R. Garcia, N. Calvo, and D. Marsh (2009), ENSO influence on zonal mean temperature and ozone in the tropical lower stratosphere, *Geophys. Res. Lett.*, *36*, L15822, doi:10.1029/2009GL039343.

Richter, J. H., F. Sassi, and R. R. Garcia (2010), Toward a physically based gravity wave source parameterization in a general circulation model, *J. Atmos. Sci.*, *67*, 136–156, doi:10.1175/2009JAS3112.1.

Sassi, F., D. Kinnison, B. A. Boville, R. R. Garcia, and R. Roble (2004), Effect of El Niño–Southern Oscillation on the dynamical, thermal, and chemical structure of the middle atmosphere, *J. Geophys. Res.*, *109*, D17108, doi:10.1029/2003JD004434.

SPARC CCMVal (2010), SPARC Report on the Evaluation of Chemistry-Climate Models, edited by V. Eyring, T. G. Shepherd, and D. W. Waugh, *WCRP-132, WMO/TD-1526, SPARC Rep. 5*, World Meteorol. Organ., Geneva, Switzerland. [Available at http://www.sparc-climate.org.]

van Loon, H., and K. Labitzke (1987), The Southern Oscillation: Part V. The anomalies in the lower stratosphere of the Northern Hemisphere in winter and a comparison with the quasi-biennial oscillation, *Mon. Weather Rev.*, *115*, 357–369, doi:10.1175/1520-0493(1987)115<0357:TSOPVT>2.0.CO;2.

Wei, K., W. Chen, and R. Huang (2007), Association of tropical Pacific sea surface temperatures with the stratospheric Holton-Tan Oscillation in the Northern Hemsiphere winter, *Geophys. Res. Lett.*, *34*, L16814, doi:10.1029/2007GL030478.

N. Calvo and D. R. Marsh, Atmospheric Chemistry Division, National Center for Atmospheric Research, PO Box 3000, Boulder, CO 80307, USA. (calvo@ucar.edu)